

Oxygen deficiency and Sn doping of amorphous Ga_2O_3

Cite as: Appl. Phys. Lett. **108**, 022107 (2016); <https://doi.org/10.1063/1.4938473>

Submitted: 24 September 2015 . Accepted: 04 December 2015 . Published Online: 14 January 2016

M. D. Heinemann , J. Berry, G. Teeter, T. Unold, and D. Cinley



[View Online](#)



[Export Citation](#)



[CrossMark](#)

ARTICLES YOU MAY BE INTERESTED IN

[A review of \$\text{Ga}_2\text{O}_3\$ materials, processing, and devices](#)

Applied Physics Reviews **5**, 011301 (2018); <https://doi.org/10.1063/1.5006941>

[Gallium oxide \(\$\text{Ga}_2\text{O}_3\$ \) metal-semiconductor field-effect transistors on single-crystal \$\beta\$ - \$\text{Ga}_2\text{O}_3\$ \(010\) substrates](#)

Applied Physics Letters **100**, 013504 (2012); <https://doi.org/10.1063/1.3674287>

[Oxygen vacancies and donor impurities in \$\beta\$ - \$\text{Ga}_2\text{O}_3\$](#)

Applied Physics Letters **97**, 142106 (2010); <https://doi.org/10.1063/1.3499306>

Lock-in Amplifiers

[Find out more today](#)



Zurich
Instruments

Oxygen deficiency and Sn doping of amorphous Ga_2O_3

M. D. Heinemann,^{1,*} J. Berry,² G. Teeter,² T. Unold,¹ and D. Ginley²

¹Helmholtz-Zentrum Berlin für Materialien und Energie, Schwarzschildstraße 3, 12489 Berlin, Germany

²National Renewable Energy Laboratory, Golden, Colorado 80401, USA

(Received 24 September 2015; accepted 4 December 2015; published online 14 January 2016)

The potential of effectively *n*-type doping Ga_2O_3 considering its large band gap has made it an attractive target for integration into transistors and solar cells. As a result amorphous GaO_x is now attracting interest as an electron transport layer in solar cells despite little information on its optoelectrical properties. Here we present the opto-electronic properties, including optical band gap, electron affinity, and charge carrier density, for amorphous GaO_x thin films deposited by pulsed laser deposition. These properties are strongly dependent on the deposition temperature during the deposition process. The deposition temperature has no significant influence on the general structural properties but produces significant changes in the oxygen stoichiometry of the films. The density of the oxygen vacancies is found to be related to the optical band gap of the GaO_x layer. It is proposed that the oxygen deficiency leads to defect band below the conduction band minimum that increases the electron affinity. These properties facilitate the use of amorphous GaO_x as an electron transport layer in $\text{Cu}(\text{In},\text{Ga})\text{Se}_2$ and in Cu_2O solar cells. Further it is shown that at low deposition temperatures, extrinsic doping with Sn is effective at low Sn concentrations. © 2016 AIP Publishing LLC. [<http://dx.doi.org/10.1063/1.4938473>]

Crystalline β - Ga_2O_3 has received considerable attention in the last few years due to promising applications in transistors and photo-detectors.^{1,2} Ga_2O_3 can also serve as a charge selective contact specifically as an electron transport layer (ETL) because of its high optical band gap combined with sufficient *n*-type doping from Sn or Si. In crystalline β - Ga_2O_3 thin films charge carrier densities above $1 \times 10^{19} \text{ cm}^{-3}$ were reported for Si and Sn doped layers.^{3,4} However, band gap and *n*-type doping of amorphous GaO_x (a- GaO_x) have not been studied.

Recently, low temperature deposited a- GaO_x has been successfully applied as an ETL in $\text{Cu}_{0.9}(\text{In}_{0.7},\text{Ga}_{0.3})_{1.1}\text{Se}_2$ (CIGS)⁵ and in Cu_2O ⁶ solar cells. This is remarkable since CIGS and Cu_2O have quite different electron affinities (EA), 4.5 eV (Refs. 7 and 8) and 3.2–4 eV,^{9,10} respectively, and therefore different requirements for the electron affinities of their ETLs. Although some changes in the band alignment can occur after formation of the hetero-junction, the electron affinity of the ETL is critical as it directly impacts the recombination losses at the p/n-junction.¹¹ If the electron affinity of the absorber material is lower compared with the ETL, it increases the interface recombination and decreases the V_{OC} ; if the EA is larger it could increase the recombination in the space charge region which reduces the fill factor. The electron affinity of stoichiometric crystalline β - Ga_2O_3 has been reported to be around 3.5–4 eV,^{12,13} which would be suitable for Cu_2O but not for CIGS. It is especially remarkable that an intentional increase of the electron affinity of a- GaO_x by the addition of indium to the a- GaO_x layer led to a reduced V_{OC} within the CIGS devices. This suggests that the electron affinity of the a- GaO_x was similar or even larger to that of CIGS. On the other hand, in organic solar cells with the low electron affinity material PCBM used as the acceptor material, β - Ga_2O_3 was shown to induce an electron barrier when used as an ETL.¹⁴ This leads to the hypothesis that the

electron affinity of a- GaO_x depends on the deposition conditions and may be higher than that of the crystalline β - Ga_2O_3 . Interestingly, the optimum a- GaO_x process conditions for the Cu_2O application was at high oxygen partial pressure of 17×10^{-3} mbar, whereas the a- GaO_x for the CIGS application was prepared under pure argon atmosphere, indicating that the resultant oxygen concentration in the films and the density of oxygen vacancies may strongly influence the electron affinity. Amorphous GaO_x that forms at the CIGS/ZnO interface in CIGS superstrate solar cells was suggested to have an electron affinity of 4.5 eV,¹⁵ based on the results of numerical device simulations. However, no reports on the measured electron affinity, charge carrier density, or oxygen deficiency of purposefully grown amorphous GaO_x exist.

In this work a- GaO_x layers are prepared by pulsed laser deposition (PLD) at various temperatures, by utilizing a temperature gradient across the substrate. The oxygen partial pressure was fixed at 2×10^{-5} mbar for the samples with a temperature gradient from 425 °C to 300 °C, and at 1.3×10^{-3} mbar for the samples with a temperature gradient from 160 °C to 100 °C; the surface temperature was measured with a calibrated IR camera. Higher oxygen partial pressures were not possible to control and lower oxygen partial pressures lead to opaque films. The surface stoichiometry was measured by x-ray photoelectron spectroscopy (XPS). Schottky devices were fabricated on ZnO:Ga (GZO) in an Au/a- GaO_x /GZO geometry and capacitance-voltage (*C*-*V*) measurements were used to extract the charge carrier density within the a- GaO_x layers and the built-in potential of the Schottky contact. The band gap was determined by transmission/reflection measurements. Layers of 10 nm thickness were deposited on GZO/alkali-free-glass substrates for the XPS measurements, while 200 nm thick layers on GZO/alkali-free-glass substrates were used for the Schottky devices and 200 nm thick layers on Quartz substrates employed for

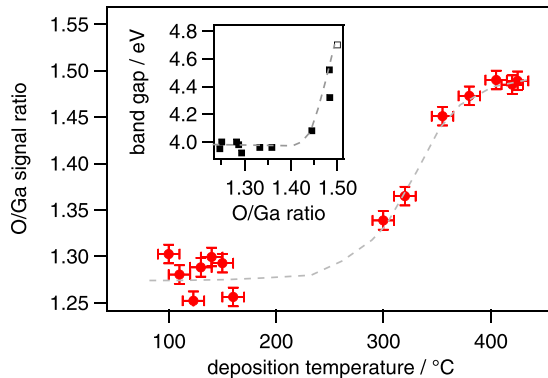


FIG. 1. Ratio of the O 1s and the Ga 2p XPS peak normalized to the Ga_2O_3 stoichiometric value of 1.5 for the highest deposition temperature. The inset shows the correlation of this O/Ga ratio and the optical band gap. The white dot is the literature value for stoichiometric $\beta\text{-Ga}_2\text{O}_3$.

the T/R measurements. Thicknesses were determined from the optical data and confirmed by mechanical profilometer measurements.

The GaO_x layers deposited by PLD displayed an amorphous structure for substrate temperatures up to 450°C during the deposition. No variations were observed in the XRD patterns below this temperature. Layers deposited above 450°C were found to have peaks for the $\beta\text{-Ga}_2\text{O}_3$ crystalline phase as reported in the literature.¹⁶ Here, the relative oxygen content of the a- GaO_x layer deposited at different substrate temperatures was measured by XPS. The ratio of the O 1s and the Ga 2p peak intensities is used as a measure and is plotted against the deposition temperature in Fig. 1. The O/Ga ratio at the high temperatures was normalized to the stoichiometric value of 1.5. Oxidation at these elevated temperatures is very effective, and the resulting films are generally close to the Ga_2O_3 stoichiometry. With decreasing deposition temperature, we observe that the O/Ga ratio decreases and becomes constant around 1.3 at temperatures below 300°C .

Together with the observed change in chemical composition, an associated change in the optical properties is shown in Fig. 2 which plots the square of the absorption coefficient of a- GaO_x layers, obtained from the T/R measurements. For direct band gaps, the value of the band gap E_g can be extracted from a linear extrapolation of α^2 to zero.¹⁷ Above 450°C the a- GaO_x crystallizes and the band gap increases to 4.7 eV, close to the value of 4.8–5 eV previously reported for $\beta\text{-Ga}_2\text{O}_3$.¹⁸ At 425°C the band gap of the layer is reduced to 4.5 eV. It further decreases for lower temperatures until it stays constant around 4.0 eV for all deposition temperatures below 320°C . This trend was also observed for the surface band gap value, which was obtained from XPS. XPS gives the energetic difference between the Fermi level (E_F) and the valence band maximum (VBM), which equals the band gap for strongly *n*-type doped materials. All films are sufficiently *n*-type doped to allow this approximation, as shown in Fig. 3. From *C*-*V*, the charge carrier density of $3 \times 10^{17} \text{ cm}^{-3}$ is obtained for the low temperature deposited films. It increases with increasing temperature up to $1 \times 10^{18} \text{ cm}^{-3}$ at 425°C . From this, the difference between the Fermi level and the conduction band minimum (CBM) can be calculated, resulting in 20 meV for $1 \times 10^{18} \text{ cm}^{-3}$ and

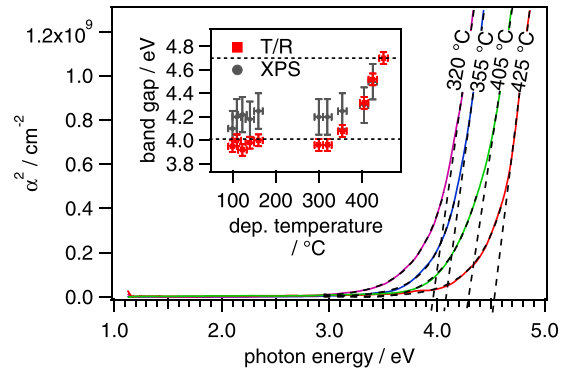


FIG. 2. Square of the absorption coefficient for a- GaO_x films deposited at different temperatures. The band gap is derived from the linear interpolation of the high-energy part, while the Urbach tail in the low energy part is fitted with an exponential function (both plotted as dashed lines). The inset compares the results with those obtained from XPS measurements.

50 meV for $3 \times 10^{17} \text{ cm}^{-3}$. This also shows that the Burstein-Moss shift is not a significant influence on the observed optical band gap. The inset of Fig. 2 shows the dependence of the measured bulk and the surface band gaps on deposition temperature. The small discrepancy observed between both may be explained by the differences of bulk and surface properties, but both show a similar trend of decreasing band gap with decreasing deposition temperature.

Further, the trend of the band gap with increasing deposition temperature is very similar to the trend of the oxygen concentration within the films. To confirm the correlation between band gap and film stoichiometry, low temperature deposited films with an optical band gap of 4.05 eV were annealed at 450°C for 1 h in air and in vacuum. The band gap of the vacuum annealed sample actually decreased to 4.02 eV, while the band gap of the air annealed sample increased to 4.40 eV. This confirms that the sub-stoichiometry, likely as a result of the low-deposition temperature, is the reason for the reduced band gap. Disorder effects as generally observed in amorphous oxides induce a high density of deep tail-states above the VBM.^{19,20} These cause strong exponentially decaying tails of the absorption coefficient towards lower photon energies,²¹ as seen in the absorption coefficient shown in Fig. 2. The tail widths can be described by the exponential decay parameter, the so-called Urbach energy. However, the Urbach energy calculated for

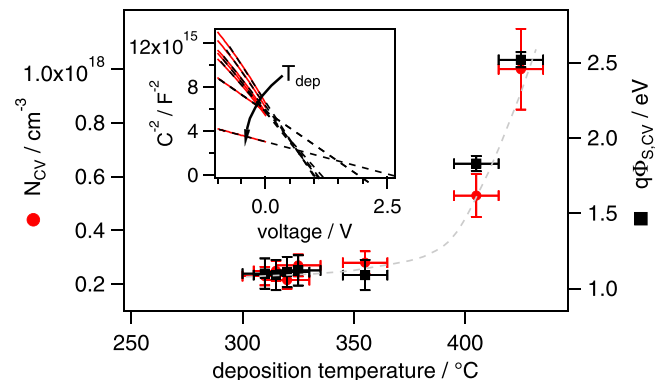


FIG. 3. Schottky barrier to Au and charge carrier density of the a- GaO_x films deposited at different temperatures. The inset shows the Mott-Schottky plots (1 kHz, 300 K) used to determine these values.

the films studied here are almost constant for the different deposition temperatures with values around 500 meV. This again indicates that the change of the optical band gap does not only originate from a change in disorder.

Based on these observations it is reasonable to hypothesize that the observed change of the band gap is induced by a change in the oxygen content within the films. It can be seen in Fig. 1 that it requires around 8% oxygen deficiency to reduce the band gap to 4 eV. The reduced band gap is then likely to be induced by a defect band created by V_O defect states. We note that in crystalline films, sub-stoichiometry was identified as the origin for strong sub-band gap absorption leading to opaque films.⁴ This was argued to be due to the formation of GaO phases. The low-temperature deposited amorphous films seem to allow such sub-stoichiometry without the formation of opaque GaO phases.

Density functional theory (DFT) calculations have predicted the V_O donor state to be at about 1 eV below the CBM in the crystalline β -Ga₂O₃ phase.²² Experimentally, three deep electron traps were found at 0.55, 0.74, and 1.04 eV below the conduction band edge.²³ This is consistent with the V_O donor states being the origin of the sub-CBM defects, increasing the electron affinity of the material. Similar effects were reported for oxygen deficient MoO₃ and SiO_x films,^{24–26} in which these defect bands are assumed to provide a channel for current transport. If this is indeed the case it should be possible to probe the defect band with electrical characterization methods. To test this, Au Schottky contacts were fabricated and measured, allowing the calculation of the electron affinity by measuring the barrier height at the Au/a-GaO_x interface. The Schottky barrier height between a-GaO_x and Au is defined by the difference of the Au work function and the electron affinity of a-GaO_x. Thus, if the band gap change is due to a change of the electron affinity, as induced by a defect band close to the CBM, the Schottky barrier between a-GaO_x and Au should change accordingly. The *J-V* curves of the Au Schottky devices are shown in Fig. 4. It can be seen that the *J-V* curves of the a-GaO_x layers deposited at different temperatures are shifted relative to one another, similar to the optical band gaps, indicating an increasing barrier with an increasing band gap. By fitting the linear slope in the semi-log plot shown in the inset of Fig. 4 with the equations given in Ref. 27, the ideality factor and the barrier height can be calculated. However, the ideality factors

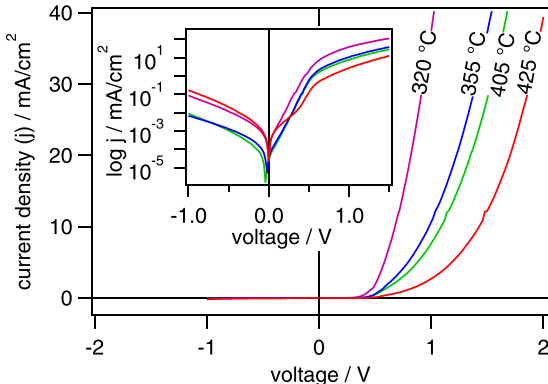


FIG. 4. *J-V* curves of the Au Schottky devices with a-GaO_x films deposited at different temperatures. The inset shows the semi-log-plot with a fit to the linear region to obtain the barrier height for thermionic emission.

obtained by this fit are larger than two, indicating complex transport through the interface barrier, likely a result of trap assisted tunneling and/or barrier inhomogeneities. The high ideality factor leads to an underestimation of the barrier height. The resulting barrier height is 730 meV for the layer deposited at 320 °C and increases up to 810 meV for the layer deposited at 425 °C. Alternatively, the barrier height can be extracted from Mott-Schottky plots.²⁸ These results are shown in Fig. 3. The barrier heights of the low-band gap layers deposited at around 320 °C are 1.1 eV, whereas the barrier height increases at deposition temperatures higher than 350 °C and reaches a maximum value of 2.5 eV at 425 °C. The difference in the values obtained from *J-V* and from *C-V* analyses may originate from lateral inhomogeneities of the barrier height or from the fact, that, due to series resistance effects, the *C-V* data had to be recorded at rather low frequencies (1 kHz), at which the capacitance could be influenced by deep defects. Also, the capacitance is recorded at reverse bias whereas the analyzed *J-V* data at forward bias. Nevertheless, both measurements show an increasing Schottky barrier with an increasing deposition temperature of the a-GaO_x layer, confirming the hypothesis that the change in the band gap results in a change of the electron affinity, due to a V_O induced defect band.

The presence of such a V_O induced defect band below the CBM also explains the different oxygen background pressures during a-GaO_x deposition needed to get good ETLs in CIGS or in Cu₂O devices. Cu₂O devices require a-GaO_x layers deposited at high oxygen partial pressure. According to the results presented here, this reduces the electron affinity to a value close to that of Cu₂O (3.2–4 eV) and lowers the interface recombination losses, just as illustrated in Fig. 5. CIGS devices require low oxygen partial pressures as the defect bands are beneficial for the electron transport from CIGS to the ZnO window layer. However further alloying with In of the a-GaO_x layer leads to a V_{OC} reduction, and thus the electron affinity of the oxygen deficient layer should

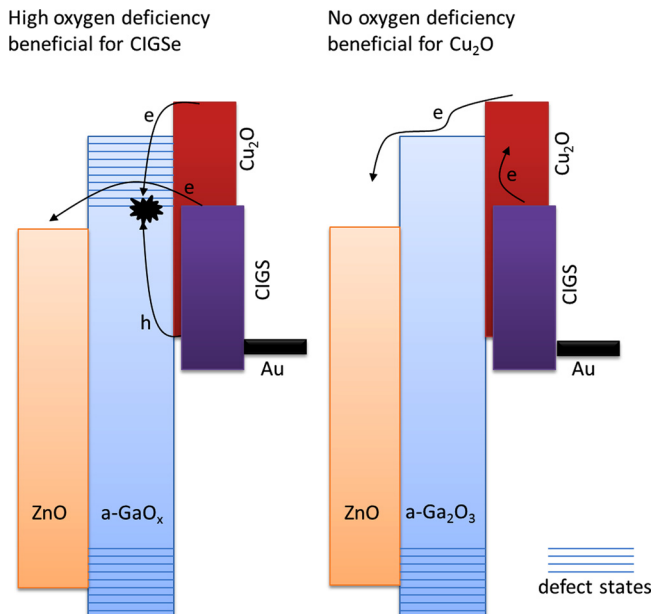


FIG. 5. Schematic drawing of a-GaO_x as an electron transport layer within CIGS and Cu₂O devices. High oxygen deficiency allows electron transport through sub-CBM defect states.

be similar or larger than the electron affinity of CIGS (4.5 eV). Thus, it is proposed that the oxygen concentration within the films can be used to adjust its electron affinity by at least 500 meV.

For the application of a-GaO_x as an ETL it is beneficial to increase the *n*-type carrier density via external doping. However, no reports exist so far on doping of a-GaO_x successfully. Recently, it was found by Siah *et al.*²⁹ that Sn dopants in low temperature deposited a-GaO_x are inactive since they are present in either Sn⁺² or Sn⁺⁴ charge states. Here we measured the charge carrier density with *C-V* on a-GaO_x samples deposited at a substrate temperature of 100 °C resulting in an optical band gap of 4 eV. The Sn concentration was varied from 0.2 at. % to 0.9 at. %, which was estimated from the ratio of the SnO₂ to Ga₂O₃ ablation pulses, weighted with the deposition thickness per pulse for SnO₂ and Ga₂O₃. The measured charge carrier density increases linearly with increasing Sn concentration from $2 \times 10^{17} \text{ cm}^{-3}$ as measured for undoped a-GaO_x to $1 \times 10^{18} \text{ cm}^{-3}$ at a Sn concentration of 0.6 at. %. For Sn concentrations above 0.6 at. % the charge carrier density drops again, possibly due to the formation of SnO₂ phases or due to an increased presence of Sn⁺² states. This indicates that it is possible to dope a-GaO_x with Sn, for sufficiently low Sn concentrations. At higher deposition temperatures it may also be possible to apply higher Sn concentrations while keeping Sn⁺⁴ the dominant charge state.

In summary, it was found that a-GaO_x layers can be grown at low temperature and low oxygen partial pressures exhibiting a strong oxygen deficiency while remaining transparent. The optical band gap of the oxygen deficient layers was found to decrease to 4 eV due to an increase of the electron affinity. It is argued that the origin of this effect is the formation of a V_O defect band. This is found to be consistent with a range of opto-electronic measurements confirming the validity of this proposed mechanism. Efficient electron transport through this defect band can also explain why a-GaO_x can be used as an efficient electron transport layer in CIGS devices. Finally it was shown that it is possible to extrinsically *n*-type dope a-GaO_x with low concentrations of Sn.

We would like to thank John Perkins for helpful discussions, Maikel van Hest for depositing the GZO films, Vincent Bollinger, Matthew Reese, Andriy Zakutayev, Paul Ndione, and Matthew Young for the technical support. This work was financially supported by the HNSEI project SO-075 of the Helmholtz Association Initiative and Network Fund.

- ¹M. Higashiwaki, K. Sasaki, A. Kuramata, T. Masui, and S. Yamakoshi, “Gallium oxide (Ga₂O₃) metal-semiconductor field-effect transistors on single-crystal beta-Ga₂O₃ (010) substrates,” *Appl. Phys. Lett.* **100**(1), 013504 (2012).
- ²T. Oshima, T. Okuno, N. Arai, N. Suzuki, S. Ohira, and S. Fujita, “Vertical solar-blind deep-ultraviolet Schottky photodetectors based on β -Ga₂O₃ substrates,” *Appl. Phys. Express* **1**(1), 011202 (2008).
- ³S. Müller, H. v. Wenckstern, D. Splith, F. Schmidt, and M. Grundmann, “Control of the conductivity of Si-doped β -Ga₂O₃ thin films via growth temperature and pressure,” *Phys. Status Solidi (A)* **211**(1), 34–39 (2014).
- ⁴M. Orita, H. Hiramatsu, H. Ohta, M. Hirano, and H. Hosono, “Preparation of highly conductive, deep ultraviolet transparent β -Ga₂O₃ thin film at low deposition temperatures,” *Thin Solid Films* **411**(1), 134–139 (2002).
- ⁵T. Koida, Y. Kamikawa-Shimizu, A. Yamada, H. Shibata, and S. Niki, “Cu(In,Ga)Se₂ solar cells with amorphous oxide semiconducting buffer layers,” *IEEE J. Photovoltaics* **5**(3), 956–961 (2015).

- ⁶T. Minami, Y. Nishi, and T. Miyata, “Effect of the thin Ga₂O₃ layer in n+-ZnO/n-Ga₂O₃/p-Cu₂O heterojunction solar cells,” *Thin Solid Films* **549**, 65–69 (2013).
- ⁷S.-H. Wei and A. Zunger, “Band offsets and optical bowings of chalcopyrites and Zn-based II–VI alloys,” *J. Appl. Phys.* **78**(6), 3846–3856 (1995).
- ⁸C. Platzer-Bjorkman, T. Torndahl, D. Abou-Ras, J. Malmstrom, J. Kessler, and L. Stolt, “Zn (O, S) buffer layers by atomic layer deposition in Cu (In, Ga) Se₂ based thin film solar cells: Band alignment and sulfur gradient,” *J. Appl. Phys.* **100**(4), 44506 (2006).
- ⁹W.-Y. Yang and S.-W. Rhee, “Effect of electrode material on the resistance switching of Cu₂O film,” *Appl. Phys. Lett.* **91**(23), 232907 (2007).
- ¹⁰S. Jeong, A. Mittiga, E. Salza, A. Masci, and S. Passerini, “Electrodeposited ZnO/Cu₂O heterojunction solar cells,” *Electrochim. Acta* **53**(5), 2226–2231 (2008).
- ¹¹T. Minemoto, T. Matsui, H. Takakura, Y. Hamakawa, T. Negami, Y. Hashimoto, T. Uenoyama, and M. Kitagawa, “Theoretical analysis of the effect of conduction band offset of window/CIS layers on performance of CIS solar cells using device simulation,” *Sol. Energy Mater. Sol. Cells* **67**(1), 83–88 (2001).
- ¹²M. Mohamed, K. Irmscher, C. Janowitz, Z. Galazka, R. Manzke, and R. Fornari, “Schottky barrier height of Au on the transparent semiconducting oxide β -Ga₂O₃,” *Appl. Phys. Lett.* **101**(13), 132106 (2012).
- ¹³K. Kikuchi, S. Imura, K. Miyakawa, M. Kubota, and E. Ohta, “Electrical and optical properties of Ga₂O₃/CuGaSe₂ heterojunction photoconductors,” *Thin Solid Films* **550**, 635–637 (2014).
- ¹⁴N. Zhou, M.-G. Kim, S. Loser, J. Smith, H. Yoshida, X. Guo, C. Song, H. Jin, Z. Chen, S. M. Yoon *et al.*, “Amorphous oxide alloys as interfacial layers with broadly tunable electronic structures for organic photovoltaic cells,” *Proc. Natl. Acad. Sci.* **112**(26), 7897–7902 (2015).
- ¹⁵M. D. Heinemann, V. Efimova, R. Klenk, B. Hoepfner, M. Wollgarten, T. Unold, H.-W. Schock, and C. A. Kaufmann, “Cu (In, Ga) Se₂ superstrate solar cells: Prospects and limitations,” *Prog. Photovoltaics: Res. Appl.* **23**(10), 1228–1237 (2015).
- ¹⁶S. Geller, “Crystal structure of β -Ga₂O₃,” *J. Chem. Phys.* **33**(3), 676–684 (1960).
- ¹⁷J. I. Pankove, *Optical Processes in Semiconductors* (Courier Corporation, 2012).
- ¹⁸H. Tippins, “Optical absorption and photoconductivity in the band edge of β -Ga₂O₃,” *Phys. Rev.* **140**(1A), A316 (1965).
- ¹⁹T. Kamiya and H. Hosono, “Material characteristics and applications of transparent amorphous oxide semiconductors,” *NPG Asia Mater.* **2**(1), 15–22 (2010).
- ²⁰K. Nomura, T. Kamiya, H. Yanagi, E. Ikenaga, K. Yang, K. Kobayashi, M. Hirano, and H. Hosono, “Subgap states in transparent amorphous oxide semiconductor, In-Ga-Zn-O, observed by bulk sensitive X-ray photoelectron spectroscopy,” *Appl. Phys. Lett.* **92**(20), 202117 (2008).
- ²¹T. Kamiya, K. Nomura, and H. Hosono, “Origins of high mobility and low operation voltage of amorphous oxide TFTs: Electronic structure, electron transport, defects and doping,” *J. Disp. Technol.* **5**(7), 273–288 (2009).
- ²²J. Varley, J. Weber, A. Janotti, and C. G. van de Walle, “Oxygen vacancies and donor impurities in β -Ga₂O₃,” *Appl. Phys. Lett.* **97**(14), 142106 (2010).
- ²³K. Irmscher, Z. Galazka, M. Pietsch, R. Uecker, and R. Fornari, “Electrical properties of β -Ga₂O₃ single crystals grown by the Czochralski method,” *J. Appl. Phys.* **110**(6), 063720 (2011).
- ²⁴M. Vasilopoulou, L. C. Palitis, D. G. Georgiadou, P. Argitis, S. Kennou, L. Sygellou, I. Kostis, G. Papadimitropoulos, N. Konofaos, A. A. Iliadis, and D. Davazoglou, “Reduced molybdenum oxide as an efficient electron injection layer in polymer light emitting diodes,” *Appl. Phys. Lett.* **98**(12), 123301 (2011).
- ²⁵S. Deb and J. Chopoorian, “Optical properties and color-center formation in thin films of molybdenum trioxide,” *J. Appl. Phys.* **37**(13), 4818–4825 (1966).
- ²⁶N. Tomozeiu, “Silicon oxide (SiO_x, 0 < x < 2): A challenging material for optoelectronics,” in *Optoelectronics-Materials and Techniques*, edited by P. Predeep (InTech, 2011).
- ²⁷S. M. Sze and K. K. Ng, *Physics of Semiconductor Devices* (John Wiley & Sons, 2006).
- ²⁸A. M. Goodman, “Metal–semiconductor barrier height measurement by the differential capacitance method—one carrier system,” *J. Appl. Phys.* **34**(2), 329–338 (1963).
- ²⁹S. C. Siah, R. E. Brandt, K. Lim, L. T. Schelhas, R. Jaramillo, M. D. Heinemann, D. Chua, J. Wright, J. D. Perkins, C. U. Segre, R. G. Gordon, M. F. Toney, and T. Buonassisi, “Dopant activation in Sn-doped Ga₂O₃ investigated by X-ray absorption spectroscopy,” *Appl. Phys. Lett.* **107**, 252103 (2015).